

PAPER • OPEN ACCESS

## Dynamic Modeling and Simulation of a Parallel Locking Mechanism

To cite this article: Chao Xiang *et al* 2019 *IOP Conf. Ser.: Earth Environ. Sci.* **300** 022116

View the [article online](#) for updates and enhancements.

# Dynamic Modeling and Simulation of a Parallel Locking Mechanism

Chao Xiang<sup>1,2</sup>, Baoren Li<sup>1</sup>, Yajun Gong<sup>2</sup>, Baoping Zeng<sup>2,\*</sup>

<sup>1</sup> School of mechanical science and engineering, Huazhong University of Science and Technology, Wuhan, China

<sup>2</sup> Wuhan Second Ship Design and Research Institute, Wuhan 430205, China

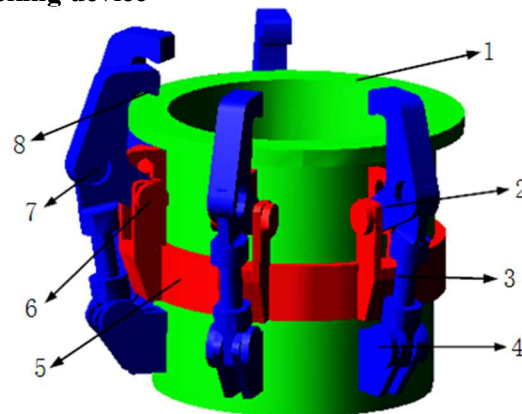
**Abstract.** Aiming at the locking problem of the mechanism in face-to-face contact, a kind of parallel mechanical locking device is designed, which can make the locked surface self-locking even when the locking hydraulic system fails, thus ensuring the safety and reliability of the locked mechanism. Through theoretical analysis and dynamic simulation of ADAMS software, the self-locking function of the device is verified and the self-locking Angle is calculated. Meanwhile, considering that the locking device may act as a "resonator" and cause secondary excitation to the locked device, which affects the vibration characteristics of the locked system, the mode analysis of the locking device is done by using ABAQUS software, and the feasibility of the locking device for the locked mechanism excited by low frequency is proved..

## 1. Introduction

With the rapid development of computer technology and the realization of unmanned office technology of automated production line, China's machinery manufacturing industry has entered a new development period [1]. Automatic locking mechanism is applied in all occupations of mechanical automation [2-3]. The locking device in contact with the surface is easy to become unstable due to the load of the locking device, which may lead to the overturn of the locking device and serious accidents. Therefore, a kind of parallel mechanical locking device is proposed, and through the dynamics simulation of ADAMS, proves that under the failure of the locking hydraulic system, the locked mechanism can still produce self-locking, which ensures the safety and reliability of the locked mechanism. Meanwhile, considering that the locking device may act as a "resonator" and cause secondary excitation to the locked device, which affects the vibration characteristics of the locked system, the mode analysis of the locking mechanism is carried out with ABAQUS, and the feasibility of the locking device is proved.



## 2. Parallel mechanical locking device



1- Locking surface; 2- Locking pawl; 3- Locking tie rod; 4 - Pin 1; 5- Locking slider; 6 - Pin 2; 7 - Pin 3; 8 – Contact Interface

**Fig. 1** A parallel mechanical locking device

As shown in Fig. 1, it is a parallel mechanical locking device with multiple locking claws. The locking slider 5 can slide on the locking base 9 under the action of the telescopic hydraulic cylinder, so that the locking claw 2 can lock or loosen the locked parts under the action of the locking rod 3. The component of 1 is the locking surface. For example, when the locking slider moves down, the contact surface 8 of the Locking claw is stitched to and pressed against the upper surface of the locking device, making the locking surface 1 and the lower surface of the locking device compressed. The contact surface 8 on the Locking claw is an inclined surface, so that when the locking hydraulic cylinder fails, the device can self-lock to ensure the safety and reliability of locking.

## 3. Self-locking function of the device

### 3.1. Analysis and calculation of self-locking principle

In order to ensure the safety and reliability of the whole locking device, the designed locking device is required to have self-locking function [4], that is, when the locking hydraulic cylinder fails, the locked mechanism can still maintain posture without toppling. The following theoretical analysis, to explain the principle of the device self-locking and derived self-locking conditions.

As shown in Fig. 2, the device is in the locking state. The force at point A is in the direction of AD rod, and the force at point C is in the direction of EC. To make the Locking claw self-locking, the resultant torque is zero or clockwise. The critical self-locking condition is that the force at point B is collinear with that at point E. That is, F1 in the figure can unlock the device, while F2 cannot. The coordinates of point A are (-260, -73.2), point B are (-160.0, 55.0), point C are (-160.0, -130.0), point D are (-210, -355), and point E are (-250, -130). Therefore, the angle between BE and the horizontal line is:

$$\text{angle} = \arctan \frac{185}{90} = 2.055 \text{rad} = 64.06 \text{deg}$$

When the angle between the resultant force direction and the horizontal line at the contact point B is less than 64.06 degrees, the device can be self-locked.

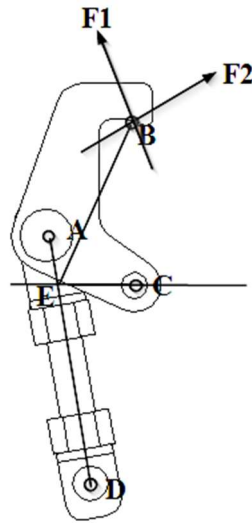


**Fig. 2** Force diagram of contact surface of locking claw

### 3.2. Dynamic simulation of self-locking function

In order to verify the correctness of the theoretical calculation, the dynamic simulation method is used in ADAMS to prove the self-locking function of the device and find the self-locking angle. The kinetic parameters involved in the modeling of locking mechanism are shown in table 1.

**Table 1** Inertia parameters of main components

Component	Mass (kg)	Moment of inertia at the center of mass		
		I <sub>xx</sub> (m <sup>2</sup> )	I <sub>yy</sub> (m <sup>2</sup> )	I <sub>zz</sub> (m <sup>2</sup> )
Locking slider	50	3.75	2.38	1.72
Locking rod	4.69	0.038	0.002	0.039
Locking claw	7.98	0.048	0.013	0.057

In order to verify the results of theoretical analysis, modeling and simulation are carried out in ADAMS, and virtual simulation method is adopted to verify the self-locking condition. The simulation method is shown in Fig. 3: without considering the influence of gravity and the failure of the locking hydraulic system, the load is carried out at point B, the constant force of  $F_x$  is maintained at 600N, and  $F_y$  starts from scratch and increases gradually. This loading method can make the total force greater than 600N and its direction from the horizontal direction to the vertical direction. The locking slider always keeps the lowest position (i.e. the locking position); When  $F_y$  reaches a certain value, the locking slider slides and reaches the highest point (i.e., the relaxed position), as shown in Fig. 4-5. It can be seen from the figure that when the y-direction force reaches 1226.8N, the device is unlocked, and the angle between the resultant force and the horizontal plane is about 64 degrees, which verifies the calculation results of the above section.

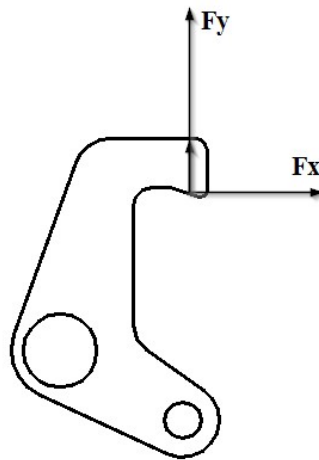


**Fig.3** Simulation verification of locking claw self-locking principle

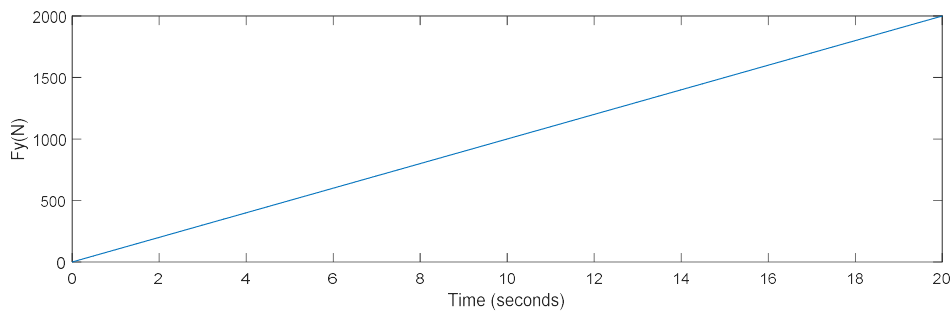


**Fig. 4** Y-direction force at point B

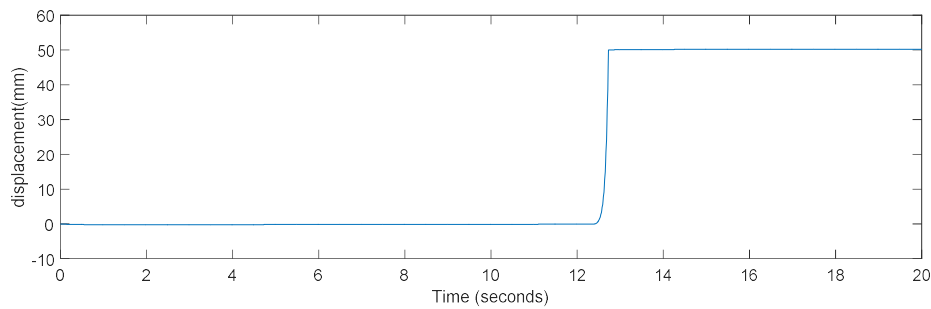


**Fig. 5** The displacement of the locking slider

After that, change the constant force of  $F_x$  at point B and conduct multiple verification. Table 2 shows the value of  $F_y$  required for unlocking under different constant forces  $F_x$ , and further the angle between the critical resultant force and the horizontal plane is calculated.

**Table 2**  $F_y$  values when unlocking under different constant forces  $F_x$

constant force of $F_x$ (N)	$F_y$ value when unlocking (N)	angle with the horizontal plane (rad)
500	1034.1	2.0582
600	1226.8	2.0546
700	1450.8	2.0652
800	1640.2	2.0502

Through repeated verification, when the reading and calculation error are ignored, it is proved that the self-locking angle of the device is about  $64^\circ$ , that is, to ensure the self-locking function, the angle between the contact surface at point B and the horizontal plane should be greater than  $26^\circ$ . After the above analysis, in order to realize the self-locking of the locking device, the inclined plane of the locking device's claw head is designed as an angle of degrees  $^\circ$  with the horizontal plane.

#### 4. Modeling and simulation of vibration characteristics of locking mechanism

The two basic elements to measure the intensity of structural vibration are frequency and amplitude respectively, and the anti-vibration performance of the structure is mainly determined by the natural frequency, stiffness and structural damping of the structure and the stiffness is generally positively correlated with its natural frequency. This section mainly analyzes the mode of the locking device [5].

##### 4.1. Establishment of finite element model of locking mechanism

Considering the solution accuracy and efficiency, the finite element calculation model of the locking device is shown in Fig. 6, including 50042 elements and 71752 nodes. According to the mechanism working principle of the locking mechanism, in ABAQUS software, the kinematic pair connection relationship between various components is established. The connection and constraint definitions of different parts are illustrated in Fig. 7. The material of the locking device is Q460 steel, and young's elastic modulus E is 200,000 MPa, poison ratio  $\mu$  is 0.3, the density  $\rho$  is  $7.849 \times 10^{-6}$  Kg/mm<sup>3</sup>.

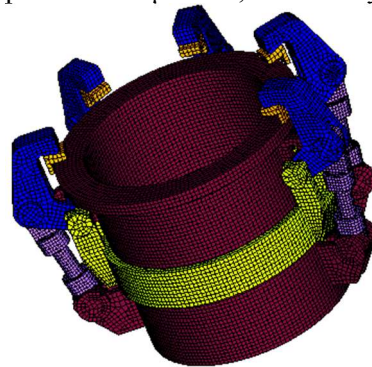


**Fig. 6** Finite element model of locking mechanism

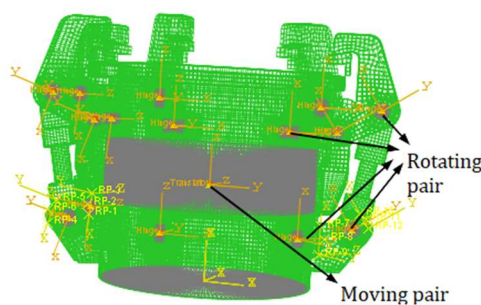


**Fig. 7** Schematic diagram of constraint definition of locking mechanism

##### 4.2. Modal analysis of locking mechanism

Modal analysis is an important method to study the vibration of multi-degree-of-freedom system and continuum system. The modal analysis method is used to understand the characteristics of each major mode of the structure in a vulnerable frequency range, to analyze the actual vibration response of the structure under the action of various internal and external vibration sources [6].

The deformation of the structure caused by gravity was taken into consideration in the modal analysis of the whole machine. After the deformation of the whole machine structure, the distribution of the

stiffness and mass of the system in space will change, thus affecting the actual mode of the system. Therefore, two analysis load steps are adopted. The first load step is only affected by gravity. The structural shape of the composite was studied. The analysis results are shown in Fig. 8. It can be seen from the figure that gravity causes certain structural deformation and establishes the connection relationship between the forces of each motion pair, which is conducive to the solution convergence of other load steps.

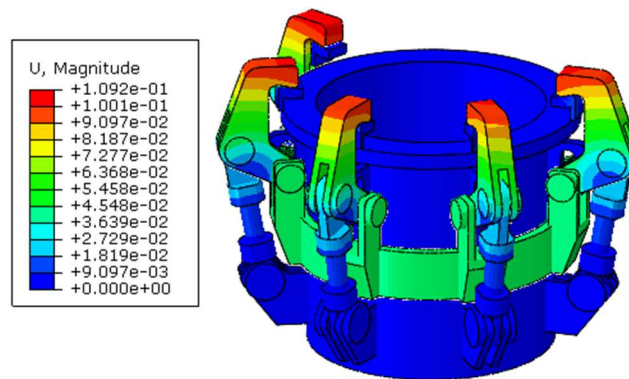


**Fig. 8** Deformation cloud diagram of locking mechanism under gravity

The second load step is modal analysis, which analyzes the modes of the system under the actual installation state. Considering the requirements of calculation cost and actual calculation accuracy, the first 60 modes of the locking mechanism are calculated. The analysis results are shown in Table 3. Due to space constraints, only a few typical results are listed here.

**Table 3** Modal analysis results of locking mechanism assembly

Modal order	modal frequency (Hz)	modal shape
1	148.29	
2	250.97	

3	259.03	<p>U, Magnitude</p> <ul style="list-style-type: none"> <li>+1.082e+00</li> <li>+9.926e-01</li> <li>+9.018e-01</li> <li>+8.117e-01</li> <li>+7.213e-01</li> <li>+6.313e-01</li> <li>+5.411e-01</li> <li>+4.509e-01</li> <li>+3.607e-01</li> <li>+2.706e-01</li> <li>+1.804e-01</li> <li>+9.018e-02</li> <li>+0.000e+00</li> </ul> <p>Max: +1.082e+00 Node: C_1.227126</p>
4	262.12	<p>U, Magnitude</p> <ul style="list-style-type: none"> <li>+1.002e+00</li> <li>+9.186e-01</li> <li>+8.351e-01</li> <li>+7.516e-01</li> <li>+6.681e-01</li> <li>+5.846e-01</li> <li>+5.010e-01</li> <li>+4.174e-01</li> <li>+3.339e-01</li> <li>+2.503e-01</li> <li>+1.667e-01</li> <li>+8.311e-02</li> <li>+0.000e+00</li> </ul> <p>Max: +1.002e+00 Node: C_1.177858</p>
5	264.68	<p>U, Magnitude</p> <ul style="list-style-type: none"> <li>+1.253e+00</li> <li>+1.134e+00</li> <li>+1.015e+00</li> <li>+8.96e-01</li> <li>+7.808e-01</li> <li>+6.656e-01</li> <li>+5.504e-01</li> <li>+4.352e-01</li> <li>+3.200e-01</li> <li>+2.048e-01</li> <li>+9.32e-02</li> <li>+0.000e+00</li> </ul> <p>Max: +1.253e+00 Node: C_1.216707</p>
6	265.93	<p>U, Magnitude</p> <ul style="list-style-type: none"> <li>+1.022e+00</li> <li>+9.363e-01</li> <li>+8.513e-01</li> <li>+7.663e-01</li> <li>+6.811e-01</li> <li>+5.959e-01</li> <li>+5.108e-01</li> <li>+4.257e-01</li> <li>+3.405e-01</li> <li>+2.554e-01</li> <li>+1.703e-01</li> <li>+8.511e-02</li> <li>+0.000e+00</li> </ul> <p>Max: +1.022e+00 Node: C_1.224378</p>
7	404.05	<p>U, Magnitude</p> <ul style="list-style-type: none"> <li>+1.079e+00</li> <li>+9.837e-01</li> <li>+8.942e-01</li> <li>+8.048e-01</li> <li>+7.154e-01</li> <li>+6.260e-01</li> <li>+5.365e-01</li> <li>+4.471e-01</li> <li>+3.577e-01</li> <li>+2.683e-01</li> <li>+1.788e-01</li> <li>+8.942e-02</li> <li>+0.000e+00</li> </ul>

As can be seen from Table 3, the natural frequency of the locking mechanism system in the assembly state is relatively high, and the first-order natural frequency is 148.29Hz. Therefore, there is no resonance for the locking mechanism excited by low frequency.

## 5. Conclusion

(1) A parallel system with multiple locking claw mechanical locking device is designed, theoretical calculation of the self-locking conditions of locking devices are deduced, namely: the angle between the contact surface of the locking claw and the horizontal plane should be greater than  $26^\circ$ . Based on the multi-body dynamics model established by ADAMS, the self-locking condition is verified. When the intersection angle is taken as  $30^\circ$ , the locking device can be self-locked. When the locking mechanism bears horizontal load, the force acting on the locking cylinder will not change no matter how big the load is. It can ensure the device in the hydraulic system failure situation still can ensure safety, will not overturn.

(2) Considering that the locking device may act as a "resonator" and cause secondary excitation to the locked device, affecting the vibration characteristics of the locked system, the mode analysis of the locking mechanism is carried out with ABAQUS software, which proves the feasibility of the locking device for the locked mechanism excited by low frequency.

## References

- [1] Wang Chunyue, Bai Haiqing, Yuan Yongliang. Optimization design of a new locking mechanism based on ADAMS [J]. Mechanism Design, 2016(7):35-38.
- [2] XU Lifeng, ZHANG Lei. Optimal Design of Dual-elbow-bar Mechanism of Die-cutting Machine Based on ADAMS. Packaging Engineering, 2013(87):75-78.
- [3] Li Taiyang, Guo Baotou, Guo Zhangxia, et al. Research and analysis of the locking device of gun reloading mechanism [J]. Ordnance Industry Automation, 2017(02):38-41.
- [4] Wu Yabei, Dou Haishi. Structure design and analysis of cage overspeed protection self-locking device [J]. Neijiang Technology, 2018, 39(09):15+43.
- [5] Ma Yonglie. Research on the realization method of structural modal analysis [D]. Zhejiang University, 2008.
- [6] Liang Le. Design and optimization of locking mechanism of space manipulator [D]. Northeastern University, 2012.